Received July 11, 2018, accepted August 18, 2018, date of publication August 28, 2018, date of current version September 28, 2018.

Digital Object Identifier 10.1109/ACCESS.2018.2867460

Two-Dimensional Direction of Arrival Estimation for Improved Archimedean Spiral Array With MUSIC Algorithm

JIN CHEN[1,2], (Member, IEEE), SHENG GUAN[1,2], YING TONG[1,2], AND LEI YAN[3]

[1]Tianjin Key Laboratory of Wireless Mobile Communications and Power Transmission, Tianjin Normal University, Tianjin 300387, China
[2]College of Electronic and Communication Engineering, Tianjin Normal University, Tianjin 300387, China
[3]Beijing Aerospace Institute for Metrology and Measurement Technology, Beijing 10076, China

Corresponding author: Ying Tong (tongying2334@163.com)

This work was supported in part by the National Natural Science Foundation of China under Grant 61701344, in part by the Tianjin Edge Technology and Applied Basic Research Project under Grant 14JCYBJC15800, in part by the Tianjin Normal University Application Development Foundation under Grant 52XK1601, in part by the Tianjin Normal University Doctoral Foundation under Grant 52XB1603 and Grant 52XB1713, and in part by the Tianjin Higher Education Creative Team Funds Program in China.

ABSTRACT Direction-of-Arrival (DOA) estimation capability of sensor arrays is greatly influenced by geometric configuration of arrays. We proposed a new type 2-D planar array, improved Archimedean spiral array (IASA), to arrange sensor elements and enhance the array performance through Archimedean curves. The 2-D MUSIC algorithm is used to estimate the spatial spectrum of signals. The analysis is complemented with numerical simulations. By comparing the root mean square error, the IASA has better 2-D DOA estimation results than circular array, rectangular array, and concentric ring array.

INDEX TERMS Sensor arrays, Spirals, Direction of arrival estimation, Planar arrays, 2-D MUSIC algorithm.

I. INTRODUCTION

Sensor array's signal processing has been widely used in many fields such as radar, sonar, and electronic reconnaissance [1]–[5]. The spectrum of time domain sequence represents the energy distribution of the signal at specific continuous frequencies. And the spatial spectrum represents the energy distribution of the signal in all directions, which is an important concept of spatial domain processing [6]. Hence, if the spatial spectrums of the signals are obtained, the Direction of Arrival (DOA) of the sources will be consequently handled and located. The high-resolution spatial spectrum estimation can accurately determine the spatial signal sources. Spatial spectrum is the superposition and extraction of spatial signals by sensor arrays. Moreover, there are several crucial factors to determine the performance of spatial spectrum estimation, such as topological structure of sensor arrays, amplitude and phase distribution of array elements, and mutual coupling effect between array elements.

At present, the researches and analyses of the spatial spectrum estimation with traditional sensor arrays have been explored and have got great achievements. Meanwhile, there are much less studies and researches of DOA with spiral arrays. The direction of arrival with logarithmic spiral array has been developed in [7], as shown in Figure 1 and their research result showed that the logarithmic spiral array has high spatial resolution.

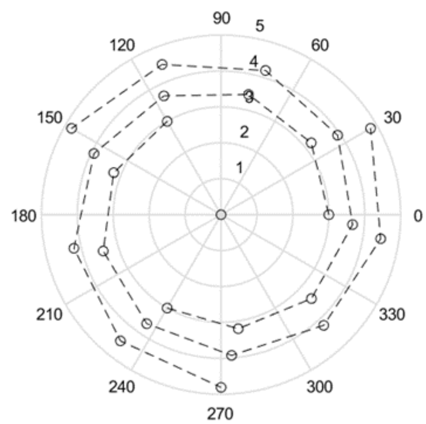

FIGURE 1. Logarithmic spiral array.

Also, Compressed Sensing algorithm was applied to thin concentric ring array in [8]. Planar array with elements obey one or several concentric rings are commonly referred to as concentric ring array. As shown in Figure 2, it shows that

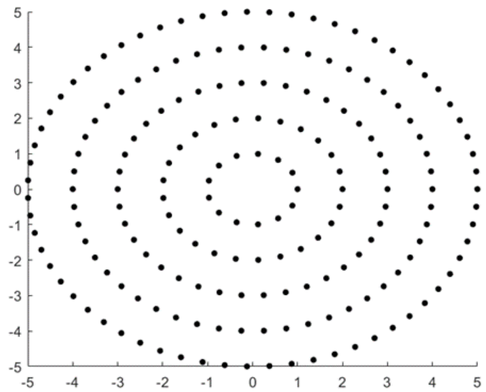

FIGURE 2. Concentric ring array.

the concentric ring array pattern has better performance and larger aperture. Due to the symmetrical structure of the ring array, the coupling effect between array elements restrained in some range. But the number of array elements increases significantly with the increase of radius of the ring, according to the relationship between the radius ρ_m and the number of elements N_m.

$$\rho_{\mathrm{m}} = (\mathrm{m}-1)\rho + \rho_1 \tag{1}$$

$$N_{\mathrm{m}} = \frac{4\pi \cdot \rho_m}{\lambda} \tag{2}$$

Where ρ is the radius of the adjacent ring, ρ_1 is the radius of the first ring, and the number of rings is represented as m.

The Archimedean spiral antennas are widely used as a kind of broad-bandwidth antennas [9]. For example, Figure 3 shows a 2-turn Archimedean spiral antenna with a 10 mm starting radius and 40 mm outer radius.

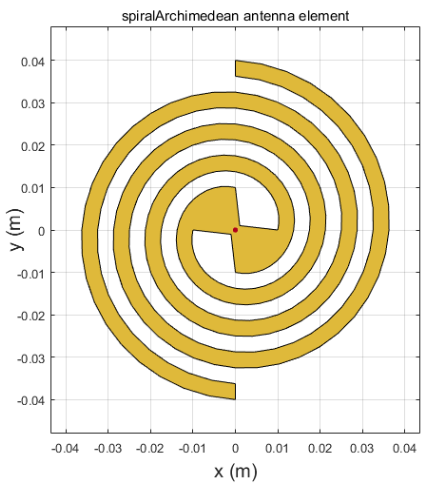

FIGURE 3. Archimedean spiral antenna.

This paper proposes a new array configuration named Improved Archimedean Spiral Array (IASA) with eight arms, which can reduce the number of array elements, restrain coupling between array elements, and improve the resolution of arrays. We applied the 2-D MUSIC algorithm to estimate the spatial spectrum. And simulation results show that the effectiveness of the IASA for spatial spectrum estimation is quite good.

We defined a narrow steering vector and the direction function in sec.2, and reviewed the 2-D DOA music algorithm in sec.3, then performed simulation in sec.4. As a result, we gave the RMSEs in different array structures, followed with conclusions in sec.5.

II. IMPROVED ARCHIMEDEAN SPIRAL ARRAY MODEL

In order to restrict the complexity of simulation, this paper is based on the following assumptions.

1). The source is a far-field signal;
2). The weight amplitudes of array elements are arranged with uniform distribution and equals to 1;
3). Ignore the Doppler effect of channel transmission;
4). Signal and noise are independent with each other;

The data model of IASA is shown in Figure 4.

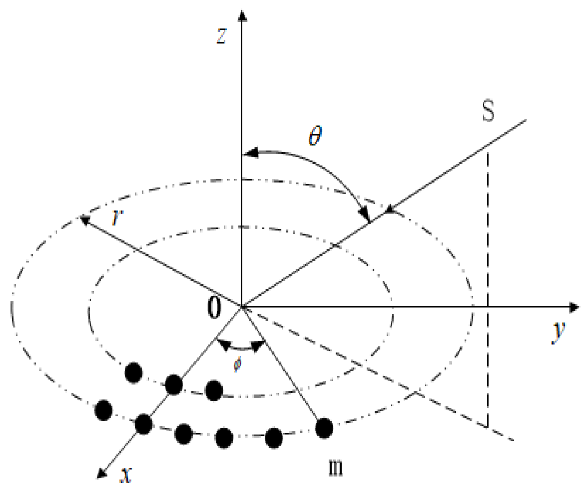

FIGURE 4. The data model of IASA.

Where the origin of the coordinate system is taken at the center O, S represents the narrowband source impinges upon the array from the far-field, $\theta \in [0, \pi/2]$ indicates the elevation angle of the source, the angle between the incident direction of the signal and the z-axis, $\phi \in [0, 2\pi]$ is the azimuth angle of the source, and this angle was set to project on the array elements plane from the x-axis with counterclockwise direction and the incident direction of the signal. According to the definition of mutual coupling between array elements, the coupling coefficient α_{ij} between the two elements is

$$\alpha_{\mathrm{ij}} = \frac{\sin(\mathrm{k} \cdot \mathrm{d_{ij}})}{\mathrm{k} \cdot \mathrm{d_{ij}}} = \mathrm{sinc}(\mathrm{k} \cdot \mathrm{d_{ij}}) \tag{3}$$

Where:

- d_{ij} are the distances between the i^{th} element and the j^{th} element;
- k is the coupling coefficient;

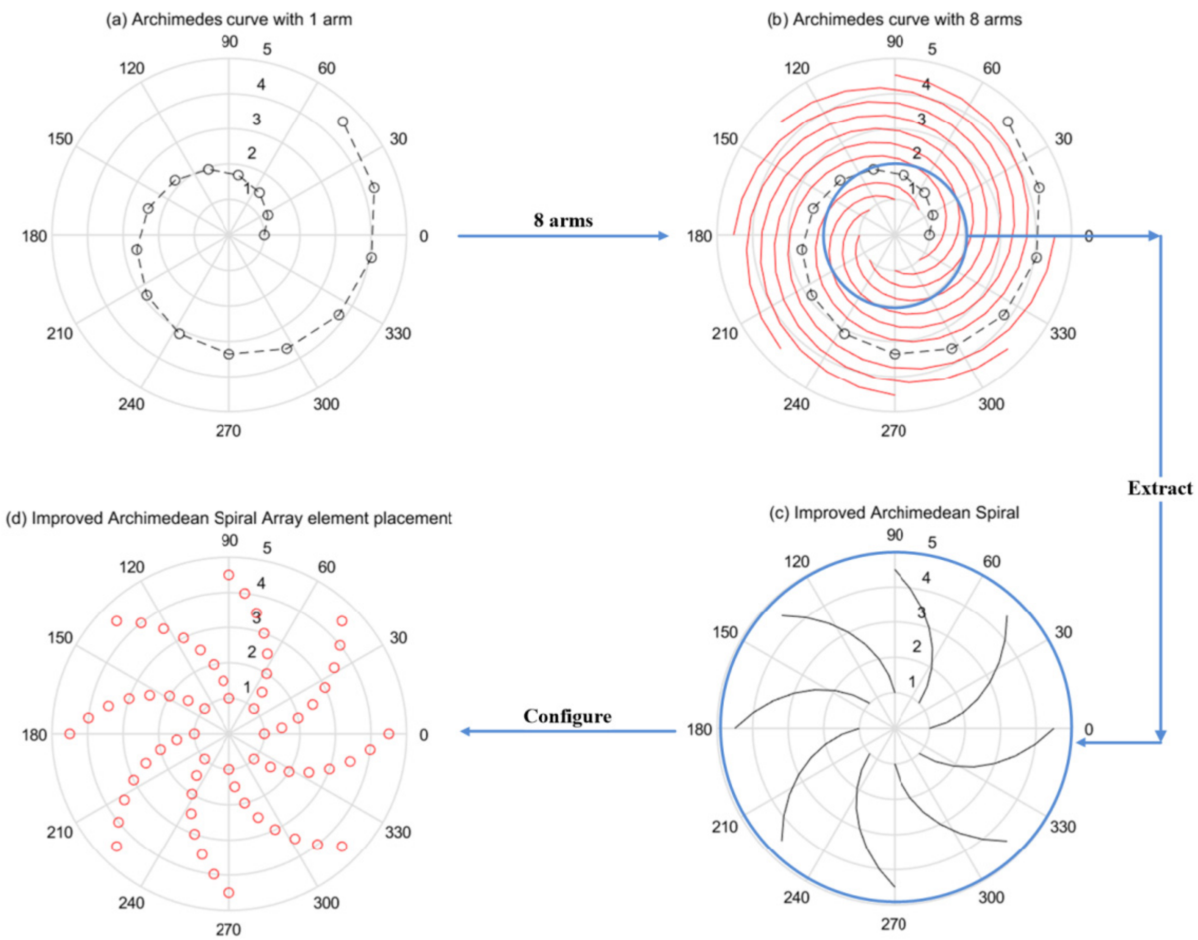

FIGURE 5. **(a)-(d) Arranging array elements through Archimedean spiral.**

And the couplings between array elements are lager while distances between elements are closer.

According to the antenna theory [10], random array element can eliminate the side lobes and expand the aperture of the array, thereby eliminating false peaks and making the array reach high resolution. The planar array structure has a circular array, a rectangular array, an L-shaped array, etc. But they are all uniform arrays. In this paper, the IASA is proposed, the details as shown in Figure 5. Because the number of array elements is small, the array elements are expanded by more than half the wavelength, which achieves the pseudo-random purpose of the array element, thereby suppressing the periodicity of the grating lobes, and at the same time The distance between the array elements increases, reducing coupling with each other. The arm radius grows linearly as a function of the winding angle.

The equation of the Archimedean spiral is:

$$r_k = a_k + b_k \cdot \theta_{k,m} \tag{4}$$

Where:

- a_k is the inner radius;
- b_k is the growth rate;
- $\theta_{k,m}$ is the winding angle of the spiral;
- k is the k^{th} arm;
- m is the m^{th} elements of the k^{th} arm;

r is the distance from a point on the helix to the origin of the coordinates, and the distance between two adjacent elements is controlled by b. The plane's Cartesian coordinate equation for the Archimedean Spiral is

$$x_{k,m} = r_k \cdot \cos(\theta_{k,m}) \tag{5}$$

$$y_{k,m} = r_k \cdot \sin(\theta_{k,m}) \tag{6}$$

The plane model of the IASA is shown in Figure 6. We discuss one of the simplest forms of configuration. Eight arms are uniformly distributed on the plane and each arms get rotation angle of 1/8 turn, $m = 8$ elements on each arms and each element rotated counterclockwise by $\pi/32$, so the number elements of the IASA is $M = 8 \times 8$, these parameters can be further optimized. The equation (4) also be written in the form

$$r_{k,m} = a_k + b_k \cdot (\frac{\pi}{32} \cdot m + (k-1) \cdot \frac{\pi}{4}) \tag{7}$$

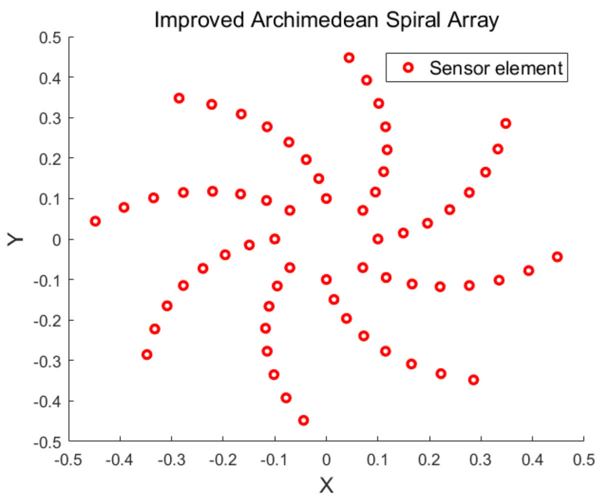

FIGURE 6. **Structure of Improved Archimedean spiral array plane model with eight arms, 1/8 turn each arm.**

In order to avoid aliasing, the $r_1 <= \lambda$ (source wavelength) has to be satisfied. In this model, we set the $r_1 = \lambda$, $r_2 = 1.5\lambda$, $r_3 = 2\lambda$, $r_4 = 2.5\lambda$, $r_5 = 3\lambda$, $r_6 = 3.5\lambda$, $r_7 = 3.5\lambda$, $r_8 = 4\lambda$, so we get the a_k and b_k. After the determination of θ, α and b, the array structure is determined,

Its position vector:

$$P_{\mathrm{k,m}} = (x_{k,m}, y_{k,m}, 0) \tag{8}$$

The direction of arrival vector:

$$\gamma_p = (\sin\theta_p \cos\phi_p, \sin\theta_p \sin\phi_p, \cos\theta_p) \tag{9}$$

Therefore, the phase difference $\Delta\psi_{k,\mathrm{m}}$ between the origin and the signal envelope received by the element m^{th} can be obtained by the dot product method:

$$\begin{aligned}\Delta\psi_{\mathrm{k},m} &= \frac{2\pi}{\lambda}\gamma_p \cdot P_{k,m} \\ &= \frac{2\pi}{\lambda} r_{k,m} \sin\theta \cos(\phi - \theta_{k,m})\end{aligned} \tag{10}$$

Assume that the main beam of the array is pointing (ϕ_0, θ_0), thus the directional function of the IASA is:

$$\begin{aligned}F(\phi,\theta) &= \sum_{k=0}^{k=7}\sum_{m=0}^{m=7} \\ &\times e^{j\frac{2\pi}{\lambda}\left(a_k + b_k\left(\frac{\pi}{32}\cdot m + (k-1)\right)\cdot\frac{\pi}{4}\right)[\sin\theta\cos(\phi-\theta_{k,m}) - \sin\theta_0\cos(\phi_0-\theta_{k,m})]}\end{aligned} \tag{11}$$

III. 2-D DOA ESTIMATION FOR ARCHIMEDEAN SPIRAL ARRAY WITH MUSIC ALGORITHM

The multiple signal classification (MUSIC) algorithm [11] is a powerful and accurate technique for determining angles of arrival in narrowband array processing application. As shown in Figure 4, the propagation of signals from P source to M sensor can be modelled by an instantaneous mixing model. The source angle is $((\phi_1, \theta_1), \cdots, (\phi_\mathrm{p}, \theta_\mathrm{p}))$, and the direction vector A can be expressed as:

$$A = \begin{bmatrix} a_{1,1}(\theta_1,\phi_1) & a_{1,1}(\theta_2,\phi_2) & \cdots & a_{1,1}(\theta_p,\phi_p) \\ \vdots & \vdots & & \vdots \\ a_{1,8}(\theta_1,\phi_1) & a_{1,8}(\theta_2,\phi_2) & \ddots & a_{1,8}(\theta_p,\phi_p) \\ \vdots & \vdots & & \vdots \\ a_{8,8}(\theta_1,\phi_1) & a_{8,8}(\theta_2,\phi_2) & \cdots & a_{8,8}(\theta_p,\phi_p) \end{bmatrix} \in C^{M\times P} \tag{12}$$

The M elements sensor array receive signal can be expressed as:

$$X = A \cdot S + V \tag{13}$$

Where $A = (\alpha_1, \alpha_2, \cdots, \alpha_P)$ is an array of steering matrix, and $S = (s_1, s_2, \cdots, s_p)$ is a matrix of signal sources, $V = (v_1, v_2, \cdots, v_p)$ representing spatially and temporally uncorrelated noise with covariance $\varepsilon[V \cdot V^{\mathrm{H}}] = \sigma^2\mathrm{I}$.

The array's second-order statistical covariance matrix $R \in C^{M\times M}$,

$$R = \frac{1}{N} X \cdot X^H \tag{14}$$

Where $\varepsilon[\cdot]$ is the expectation operation. $[\cdot]^{\mathrm{H}}$ is the conjugate transpose, N is the number of time domain snapshots, and the eigenvalue decomposition is performed on the covariance matrix R to obtain mutually orthogonal noise subspace Q_n and signal subspace Q_s,

$$R = \begin{bmatrix} Q_s & Q_n \end{bmatrix} \begin{bmatrix} \Lambda_s & \\ & \Lambda_n \end{bmatrix} \begin{bmatrix} Q_S^H \\ Q_n^H \end{bmatrix} \tag{15}$$

The idea of the MUSIC algorithm is to scan the noise subspace Q_n, The resulting signal space spectrum,

$$P(\phi,\theta)_{MUSIC} = \frac{1}{a_{\phi,\theta}^H Q_n Q_n^H a_{\phi,\theta}^H} \tag{16}$$

IV. SIMULATIONS AND RESULTS

To assess the performance of IASA at the arrival angle estimate, we performed the following simulations and compared the RMSE of IASA with circular array, rectangular array and concentric ring array.

A. 2-D DOA ESTIMATION

Example 1: Assuming the signal source is Gaussian signal with zero mean $P = 2$, snapshots is $N = 512$, signal-to-noise ratio SNR=[20,20], $\phi = [120, 250]$, $\theta = [30, 60]$, respectively. The result of the power spectrum is [103.3, 101.8] dB in Figure 7.

Example 2: If instead of the above situation, the sources located at $\phi = [120, 122]$, $\theta = [30, 32]$, respectively, the result of the power spectrum is [102.5, 102.7] dB in Figure 8.

Example 3: The source is two Gaussian coherent signal located at $\theta = [30, 60]$, $\phi = [120, 250]$, respectively.

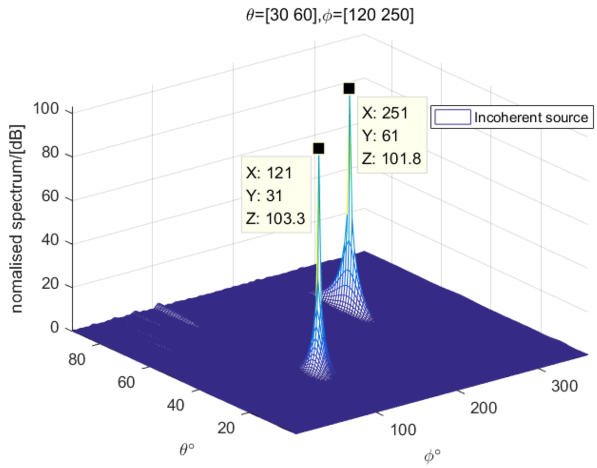

FIGURE 7. IASA spatial spectrum estimation.

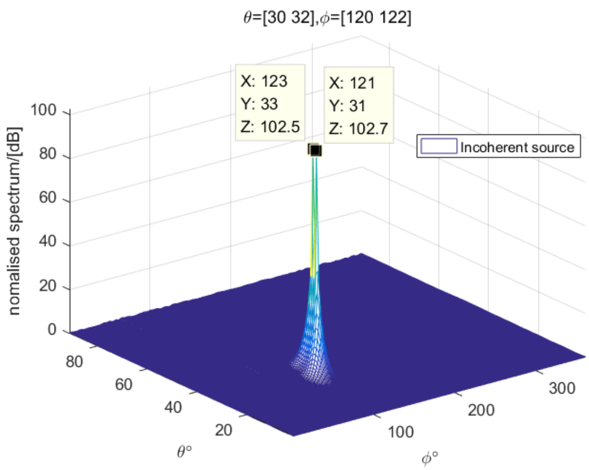

FIGURE 8. IASA spatial spectrum estimation.

SNR = [20, 20], the results of power spectrum [6.3, 6.3] dB in Figure 9.

B. PERFORMANCE METRICS

We present the Monte-Carlo simulations to assess 2-D DOA estimation performance of the proposed array. The number of Monte-Carlo estimation simulations is 100. There are two signals $L = 2$,

- source 1- located at [30.62, 30.62]
- source 2- located at [50.52, 60.52]

and the number of snapshots are $N = 256$, Comparing the circular array ($M = 64$), rectangular array ($M = 8 \times 8$) and concentric ring array (8-turn, 8 elements per turn) with proposed array, the results of RMSE is shown in Figure.8. The definition of Root Mean Squared Error (RMSE) is

$$\mu_{RMSE}(\theta_L) = \frac{1}{\mathrm{L}} \cdot \sum_{L=1}^{L} \sqrt{\frac{1}{100} \sum_{n=1}^{100} (\hat{\theta}_{L,n} - \theta_{L,n})^2} \tag{17}$$

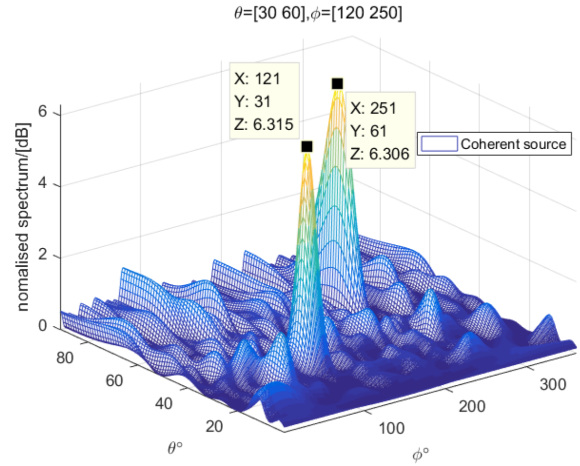

FIGURE 9. IASA spatial spectrum estimation.

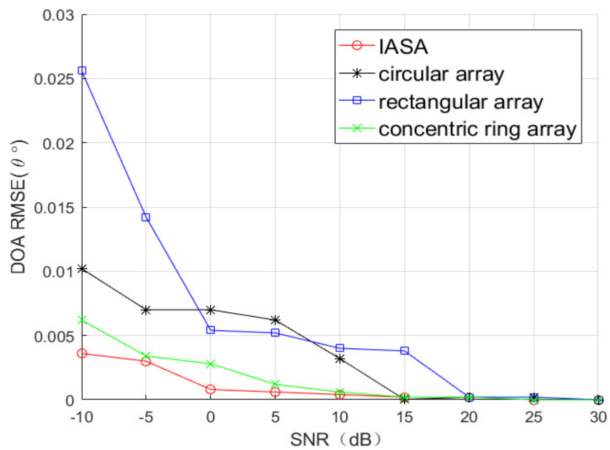

FIGURE 10. RMSEs v.s. SNR of elevation angle.

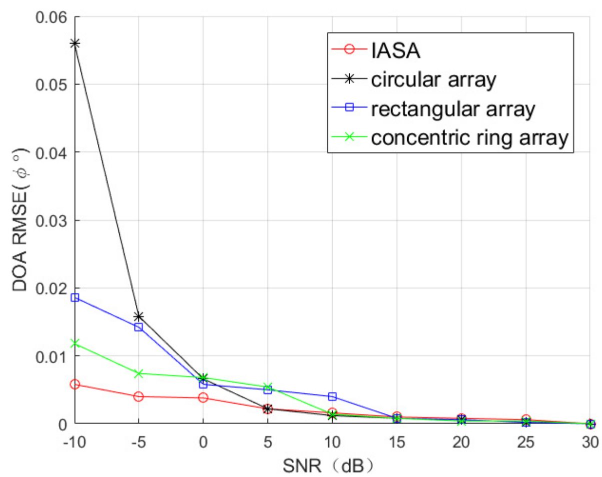

FIGURE 11. RMSEs v.s. SNR of azimuth angle.

and

$$\mu_{RMSE}(\phi_L) = \frac{1}{\mathrm{L}} \cdot \sum_{L=1}^{L} \sqrt{\frac{1}{100} \sum_{n=1}^{100} (\hat{\phi}_{L,n} - \phi_{L,n})^2} \tag{18}$$

Where $\theta^{\wedge}_{L,\mathrm{n}}$ and $\phi^{\wedge}_{L,n}$ is the estimate of the elevation angle $\theta_{L,n}$ and the azimuth angle $\phi_{L,n}$ of the n$^{\mathrm{th}}$ Monte-Carlo simulations, respectively.

V. CONCLUSION

In this paper, a new type of array topology is proposed and the simulation results are presented. The effectiveness of IASA is improved, high resolution spatial spectrum estimation, high output gain and lower RMSE are also achieved, as shown in Figure 10 and Figure 11. Note that in the degenerate case of the Gaussian coherent sources. And the robustness of the array structure at low signal-to-noise ratio provides a valuable reference for engineering applications in practice.

This paper studied the narrowband signal sources, the broadband sources need to be further explored. In addition, a 2-D nested cylindrical sensor network has been studied and presented in [12] and [13], simulation results showed that the 2-D sparse cylindrical sensor network could achieve highest resolution with fewer elements. Nested spiral array need to be further explored.

REFERENCES

[1] M. Crocco and A. Trucco, "The synthesis of robust broadband beamformers for equally-spaced linear arrays," *J. Acoust. Soc. Amer.*, vol. 128, no. 2, pp. 691–701, Aug. 2010.

[2] N. W. Bikhazi and M. A. Jensen, "The relationship between antenna loss and superdirectivity in MIMO systems," *IEEE Trans. Wireless Commun.*, vol. 6, no. 5, pp. 1796–1802, May 2007.

[3] J. O. Fiedler, K. A. Kasper, and R. W. De Doncker, "Calculation of the acoustic noise spectrum of SRM using modal superposition," *IEEE Trans. Ind. Electron.*, vol. 57, no. 9, pp. 2939–2945, Sep. 2010.

[4] J. Jia-Jia, D. Fa-Jie, and W. Xian-Quan, "A universal two-dimensional direction of arrival estimation method without parameter match," *IEEE Sensors J.*, vol. 16, no. 9, pp. 3141–3146, May 2016.

[5] S.-H. P. Won, W. W. Melek, and F. Golnaraghi, "A Kalman/particle filter-based position and orientation estimation method using a position sensor/inertial measurement unit hybrid system," *IEEE Trans. Ind. Electron.*, vol. 57, no. 5, pp. 1787–1798, May 2010.

[6] Y. J. Zhao, D. H. Li, C. Zhao, D. X. Hu, and C. C. Liu, "Basis of spatial spectrum estimation," in *Wideband Array Signal Direction of Arrive Estimation Theory and Methods*, 1st ed. Beijing, China: National Defend Industry Press, Aug. 2013, ch. 2, sec. 2, pp. 21–64.

[7] G. Hua, Y. H. Dong, and W. Hong, "Direction of arrival estimation based on logarithm spiral array," *Chin. J. Radio Sci.*, vol. 24, no. 6, pp. 987–991, 2009.

[8] X. W. Zhao, "Study of sparse array antenna synthesis based on compressed sensing and invasive weed optimization," Ph.D. dissertation, Dept. Elect. Micro., Univ. Chin. Acad. Sci., Beijing, China, 2016.

[9] S. Rupčić, V. M. Radivojević, and K. Grgić, "Loxodromic antenna arrays based on archimedean spiral," *Int. J. Elect. Comput. Eng. Syst.*, vol. 7, no. 1, pp. 7–14, 2016.

[10] B. D. Steinberg, *Microwave Imaging With Large Antenna Arrays: Radio Camera Principles and Techniques*. New York, NY, USA: Wiley, 1983, pp. 28–64.

[11] R. O. Schmidt, "Multiple emitter location and signal parameter estimation," *IEEE Trans. Antennas Propag.*, vol. AP-34, no. 3, pp. 276–280, Mar. 1986.

[12] N. Wu, F. Zhu, and Q. Liang, "Evaluating spatial resolution and channel capacity of sparse cylindrical arrays for massive MIMO," *IEEE Access*, vol. 5, pp. 23994–24003, 2017.

[13] S. Yuan and Q. Liang, "3D nested distributed massive MIMO: Modeling and performance analysis," *Ad Hoc Netw.*, vol. 58, pp. 6–12, Apr. 2017.

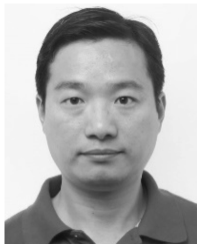

JIN CHEN was born in Wuhu, China, in 1976. He received the M.S. degree from Tianjin Normal University and the Ph.D. degree from Tianjin University, in 2005 and 2013, respectively. Since 2005, he has been with Tianjin Normal University. He is currently an Associate Professor with the Tianjin Key Laboratory of Wireless Mobile Communications and Power Transmission. His research interests include acoustic signal acquisition and processing, broadband sensor array signal processing, and artificial intelligence.

SHENG GUAN was born in Jilin, China, in 1993. He received the B.S. degree from the Inner Mongolia University of Technology in 2017. He is currently pursuing the M.S. degree with Tianjin Normal University. His research interests include signal processing and wireless communication.

YING TONG was born in Tianjin, China, in 1982. She received the B.S. and M.S. degree from Tianjin Normal University in 2004 and 2007, respectively, and the Ph.D. degree from Tianjin University in 2015. Since 2007, she has been with Tianjin Normal University, China. She is currently a Lecturer with the Tianjin Key Laboratory of Wireless Mobile Communications and Power Transmission. Her research interests include computer vision and digital signal processing.

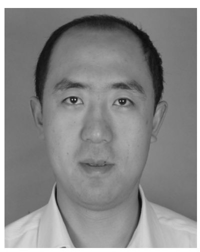

LEI YAN was born in Hohhot, China, in 1980. He received the M.S degree from Beihang University in 2007. Since 2007, he has been with the Beijing Aerospace Institute for Metrology and Measurement Technology. His research interests include high intensity sound measurement and calibration, beamforming-based microphone array measurement, and array signal acquisition and analysis. He is a Senior Engineer and a member of the China Acoustics Metrology Technical Committee.